



## Nanoparticles Ni and NiO: Synthesis, characterization and magnetic properties

Fatemeh Davar<sup>a</sup>, Zeinab Fereshteh<sup>a</sup>, Masoud Salavati-Niasari<sup>a,b,\*</sup>

<sup>a</sup> Institute of Nano Science and Nano Technology, University of Kashan, Kashan, P.O. Box 87317-51167, Islamic Republic of Iran

<sup>b</sup> Department of Chemistry, Faculty of Science, University of Kashan, Kashan, P.O. Box 87317-51167, Islamic Republic of Iran

### ARTICLE INFO

#### Article history:

Received 19 July 2008

Received in revised form

15 September 2008

Accepted 20 September 2008

Available online 7 November 2008

#### Keywords:

Nanoparticles

Ni

Inorganic materials

Characterization methods

Chemical synthesis

### ABSTRACT

The present investigation reports, the novel synthesis of nanoparticles Ni and NiO using thermal decomposition and their physicochemical characterization. The nanoparticles Ni powder have been prepared using [bis(2-hydroxyacetophenato)nickel(II)] as precursor. Transmission electron microscopy (TEM) analysis was demonstrated nanoparticles Ni with an average diameter of about 14–22 nm. The products were characterized by X-ray diffraction (XRD), TEM, high-resolution transmission electron microscopy (HRTEM) and Fourier transform infrared (FT-IR) spectroscopy. The magnetic property of Ni and NiO was studied with vibrating sample magnetometer (VSM).

© 2008 Elsevier B.V. All rights reserved.

### 1. Introduction

Nanostructured materials have been extensively explored for the fundamental scientific and technological interests in accessing new classes of functional materials with unprecedented properties and applications [1–3]. Magnetic nanoparticles are being used widely in conducting paints [4], rechargeable batteries [5,6], chemical catalysts [7], optoelectronics [8], magnetic recording media [9], ferro-fluids [10], magnetic resonance imaging contrast enhancement and drug delivery [11–13], and so on.

Nickel is one of the transition metals that exhibit magnetism as bulk material and other interesting properties and applications, such as in hydrogen storage and catalysis. Methods to produce Ni nanoparticles can be found in the literature and involve electrochemical reduction [14], chemical reduction [15,16], and sol-gel [17]. Recently, the use of organometallic precursors has been proven interesting since it leads to particles with controlled size, surface coordination, and crystallinity that are monodisperse to  $\pm 1$  atomic shell [18].

Among the transition metal magnetic nanoparticles, nickel nanocrystals are difficult to be prepared because they are eas-

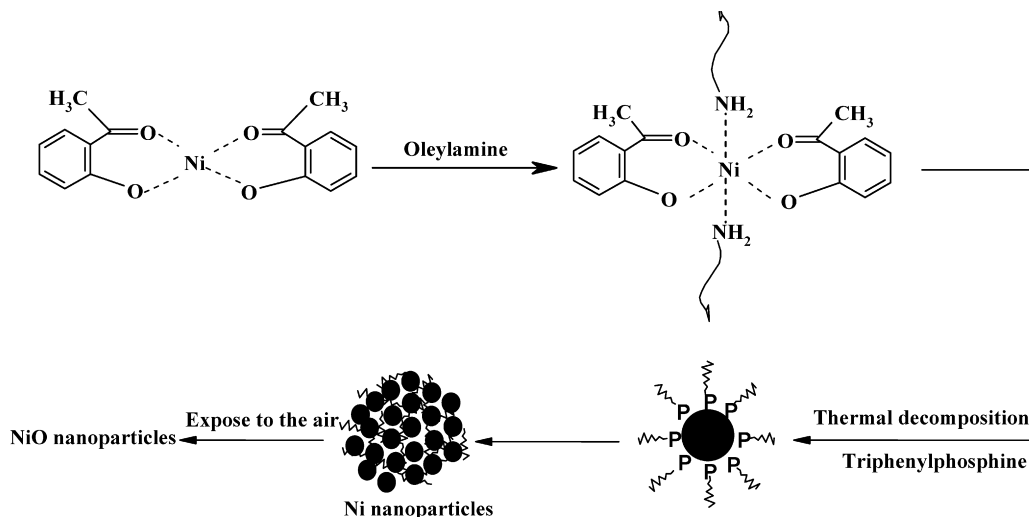
ily oxidized. To obtain pure nickel nanocrystals, many methods were performed in organic media to avoid the formation of oxide or hydroxide. Organometallic precursors, such as  $\text{Ni}(\text{CO})_4$  and  $\text{Ni}(\text{Cp})_2$ , have been used for the synthesis of nickel nanoparticles [19], and  $\text{Ni}(\text{COD})_2$  was also used to synthesize nickel particles by spontaneous decomposition in  $\text{CH}_2\text{Cl}_2$  in the presence of poly(vinylpyrrolidone) [20,21]. Nickel oxide nanoparticles have been synthesized via thermal decomposition  $\text{NiC}_2\text{O}_4$  at  $450^\circ\text{C}$  [22]. Zhang et al. [23] synthesized Ni nanocrystals with diameters in the range of 20–60 nm through decomposition of nickel acetylacetonate in oleylamine.

Among various techniques developed for the synthesis of nickel and nickel oxide nanoparticles, thermal decomposition is a novel method to produce stable monodispersed [24] and it is a rapidly developing research area. As compared to conventional method, it is much faster, cleaner and economical. However, an improvement in the thermal reduction process should be made in preparing nickel nanoparticles with controllable size and shape in order to extend the application areas and satisfy the needs of fundamental research.

The current synthetic procedure is a modified version of the method developed by Hyeon group for the synthesis of various nanoparticles of metals and oxides, which employ the thermal decomposition of metal-surfactant complexes in hot surfactant solution [25]. Recently, our groups reported the synthesis of metal oxide nanoparticles via thermal decomposition [26,27]. A major interest at the moment is in the development of organometallic

\* Corresponding author at: Institute of Nano Science and Nano Technology, University of Kashan, Kashan, P.O. Box 87317-51167, Islamic Republic of Iran. Tel.: +98 361 5555333; fax: +98 361 5552935.

E-mail address: [salavati@kashanu.ac.ir](mailto:salavati@kashanu.ac.ir) (M. Salavati-Niasari).



**Scheme 1.** Schematic diagram illustrating the formation of NiO nanoparticles.

or inorganic compound for preparation of nanoparticles. Using of the novel compound can be useful and open a new way for preparing nanomaterials to control nanocrystal size, shape and distribution size. We synthesized Ni nanoparticles from the thermal decomposition of new precursor nickel 2-hydroxyacetophenato in oleylamine (Scheme 1). In this process, oleylamine was used as both the medium and the stabilizing reagent. To the best of our knowledge, this is the first report on the synthesis of Cu nanoparticles from  $[\text{Ni}(\text{aceto})_2]$  (aceto = 2-hydroxyacetophenato). The aim of the present work is to prepare nanocrystals Ni using thermal reduction method and its physicochemical characterization.

## 2. Experimental

### 2.1. Materials

The precursor complex,  $[\text{bis}(2\text{-hydroxyacetophenato})\text{nickel}(\text{II})]$ , was prepared according to the procedure described previously [28]. Oleylamine, triphenylphosphine (TPP), toluene, hexane, and ethanol were purchased from Aldrich and used as received.

### 2.2. Characterization

XRD patterns were recorded by a Rigaku D-max C III, X-ray diffractometer using Ni-filtered  $\text{Cu K}\alpha$  radiation. Elemental analyses were obtained from Carlo ERBA Model EA 1108 analyzer. Transmission electron microscopy (TEM) images and electronic diffraction (ED) pattern were obtained on a Philips EM208 transmission electron microscope with an accelerating voltage of 200 kV. The high-resolution transmission electron microscopy (HRTEM) image and energy dispersive X-ray (EDX) were recorded on a JEOL-2010 TEM at an acceleration voltage of 200 kV. The compositional analysis was done by energy dispersive X-ray (EDX, KeveX, Delta Class I). Fourier transform infrared (FT-IR) spectra were recorded on Shimadzu Varian 4300 spectrophotometer in KBr pellets. The electronic spectra of the complexes were taken on a Shimadzu UV-vis scanning spectrometer (Model 2101 PC). The magnetic measurement was carried out in a vibrating sample magnetometer (VSM) (BHV-55, Riken, Japan) at room temperature.

### 2.3. Synthesis of Ni nanoparticles

In this synthesis, Ni nanoparticles were prepared by the thermal reduction of  $[\text{Ni}(\text{aceto})_2]$ -oleylamine complex as precursor. First, the  $[\text{Ni}(\text{aceto})_2]$ -oleylamine complex was prepared by reaction 0.5 g of  $[\text{Ni}(\text{aceto})_2]$  and 5 mL of oleylamine. The mixed solution was placed in a 50 mL three-neck distillation flask and heated up to  $150^\circ\text{C}$  for 60 min under an argon atmosphere. The resulting metal-complex solution was injected into 5 g of triphenylphosphine, TPP, at  $245^\circ\text{C}$ . As the thermal reduction proceeded, the green solution turned to black, indicating that colloidal products were generated. The black solution was aged at  $235^\circ\text{C}$  for 40 min, and was then cooled to room temperature. The black powders were precipitated by adding excess ethanol to the solution. The final products were washed with ethanol for at least three times to remove impurities, if any, and dried at  $100^\circ\text{C}$ . This product could

easily be re-dispersed in nonpolar organic solvents, such as hexane or toluene and oxidized in air (Scheme 1).

## 3. Results and discussion

The XRD pattern of the fresh nickel nanoparticles, shown in Fig. 1a, shows the face-centered cubic (fcc) structure of nickel. The peaks are extremely broad. Three characteristic peaks at  $44.58^\circ$ ,  $51.9^\circ$ , and  $76.54^\circ$  for fcc nickel (JCPDS, no. 03-1051) marked by their

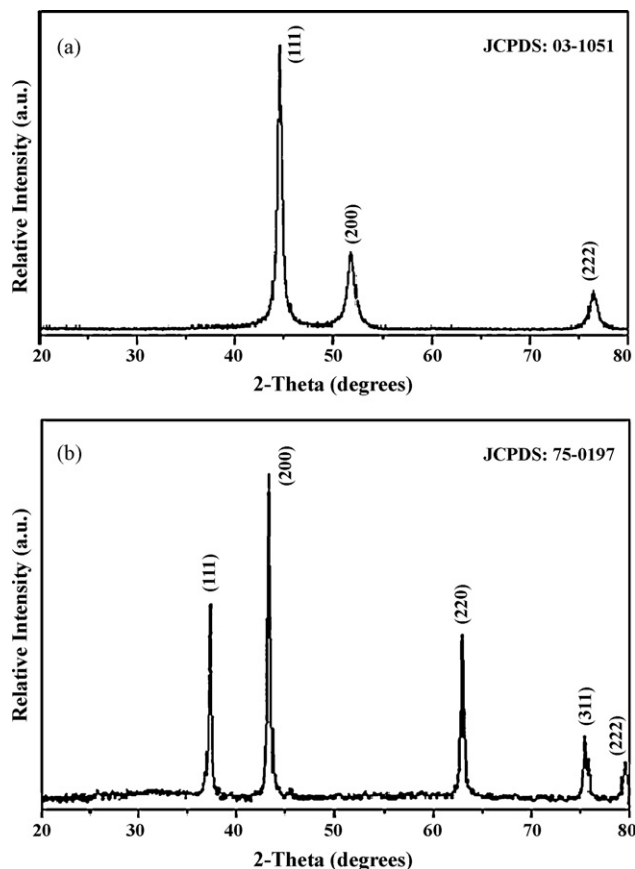


**Fig. 1.** XRD patterns of the (a) Ni and (b) NiO nanoparticles.

indices (1 1 1), (2 0 0) and (2 2 2) were observed. This revealed that the as-synthesized nanocrystals were pure nickel.

The crystallite sizes of the as-synthesized nickel,  $D_c$ , was calculated from the major diffraction peaks of the base of (1 1 1) using the Scherrer formula (Eq. (1)):

$$D_c = \frac{K\lambda}{\beta \cos \theta} \quad (1)$$

where  $K$  is a constant (ca. 0.9) [26];  $\lambda$  is the X-ray wavelength used in XRD (1.5418 Å);  $\theta$  is the Bragg angle;  $\beta$  is the pure diffraction broadening of a peak at half-height, that is, broadening due to the crystallite dimensions. The diameter of the nanoparticles calculated by the Scherrer formula is 14 nm. The XRD pattern after exposing the nanoparticles to air for than 48 h showed a NiO structure (Fig. 1b), demonstrating that the initially synthesized metallic-nickel nanoparticles were readily oxidized to NiO nanoparticles. The X-ray photoelectron spectroscopy (XPS) spectrum of the nanoparticles after air exposure revealed the NiO electronic structure rather than the metallic-nickel structure, confirming the XRD data.

FT-IR spectroscopy is a useful tool to understand the functional group of any organic molecule (Fig. 2a–c). The presence of oleylamine group on Ni nanoparticles (Fig. 2b) is indicated by the N–H wagging mode from 650 to 900  $\text{cm}^{-1}$ ;  $\text{NH}_2$  bending modes at 909, 964 and 993  $\text{cm}^{-1}$ ; and  $\text{NH}_2$  scissor mode at 1568  $\text{cm}^{-1}$  [29]. The spectrum shown in Fig. 2b also reveals the characteristic peak of the C–N stretch at 1042  $\text{cm}^{-1}$  which suggests that the C–N bonds in amine groups, and therefore oleylamine ligands, remain intact, capping the Ni nanoparticles. The peak at 1468  $\text{cm}^{-1}$  is associated with the C–H bending mode and the two peaks at 2865 and 2921  $\text{cm}^{-1}$  represent the C–H stretching modes of the oleylamine carbon chain. The presence of various N–H peaks suggests that amines are bound to the surface of the Ni nanoparticles. Based on the FT-IR data, we deduce the following reaction mechanism. Upon injection of  $[\text{Ni}(\text{aceto})_2]$  and oleylamine into hot TPP solution, the Ni–O bond is cleaved by the oleylamine group and Ni is subsequently reduced. The weak peaks at 3435  $\text{cm}^{-1}$  has been assigned to the EtOH used in the separation step. The presence of various N–H peaks suggests that amines are bound to the surface of the Ni nanoparticles. There was no evidence of free precursor, nickel 2-

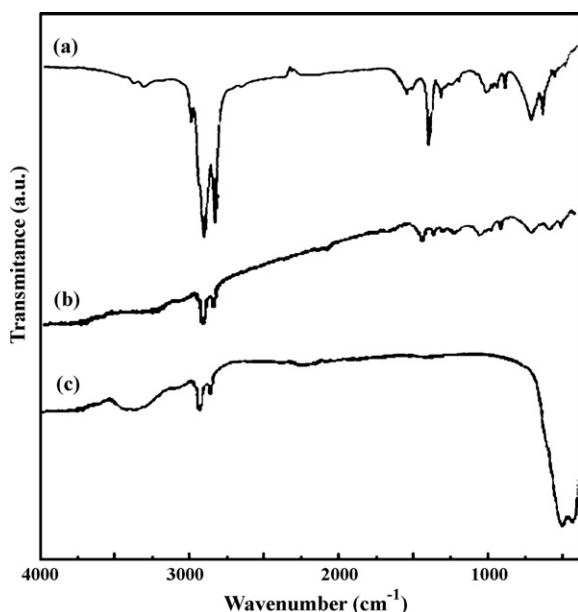


Fig. 2. FT-IR spectra of (a) oleylamine (b) Ni nanoparticles and (c) NiO nanoparticles.

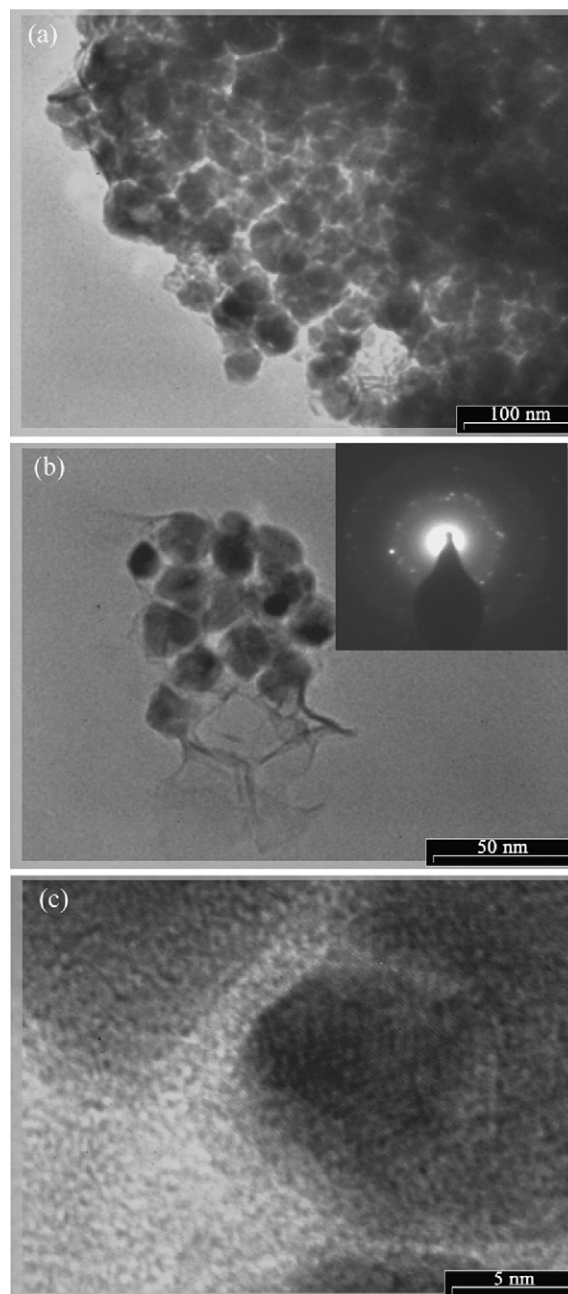


Fig. 3. (a and b) TEM images of sample (the inset shows the ED pattern) and (c) HRTEM image of the sample.

hydroxyacetophenato, in the sample, because stretch vibration of  $\text{C}=\text{O}$  ( $\nu_{\text{C}=\text{O}}$ ) and  $\text{C}-\text{O}$  ( $\nu_{\text{C}-\text{O}}$ ) disappeared. So the oleylamine serves as the capping ligand that controls growth. Fig. 2c shows that the surface was oxidized because the sample was exposed to air and some water was adsorbed probably on the external surface of the samples during handling to record the spectra. Two new peaks were shown at 445 and 490  $\text{cm}^{-1}$  in spectrum (Fig. 2c). These peaks were undoubtedly assigned to Ni–O stretching as was reported at literature [30].

Transmission electron microscopic (TEM) photographs of the product have been given in Fig. 3a. The sizes of nanocrystals obtained from the XRD diffraction patterns are in close agreement with the TEM studies which show sizes of 14–22 nm (Fig. 3a and b). These sizes are nearly spherical. We may consider that when the

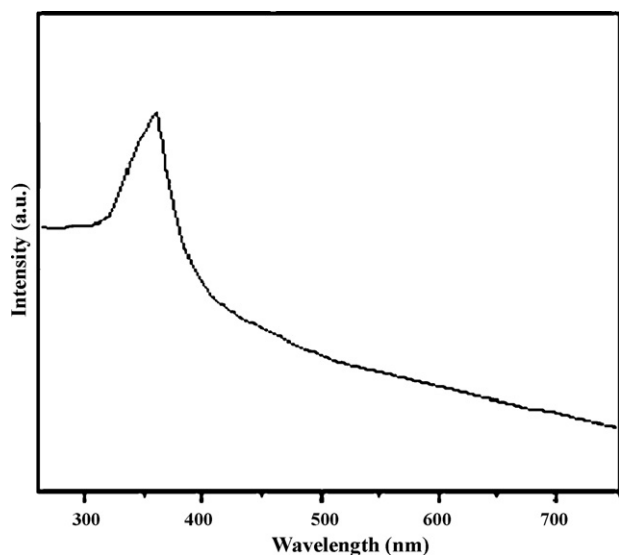


Fig. 4. UV-vis absorption spectrum of the NiO nanoparticles.

reaction was carried out at 245 °C, most organic molecules were decomposed. Since only a few oleylamine molecules were adsorbed on Ni nanoparticles. The ED pattern (Fig. 3b) indicates that the Ni nanoparticles are single-crystalline. This high-resolution TEM

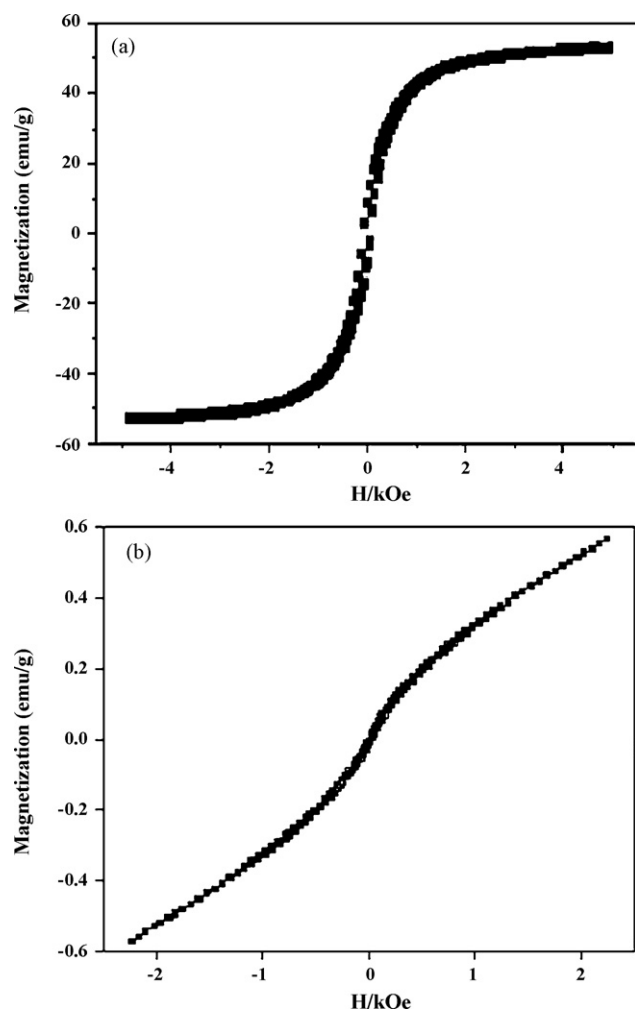


Fig. 5. Magnetization versus applied at 300 K for (a) Ni and (b) NiO nanoparticles.

(HRTEM) image of the nanoparticles revealed the highly crystalline nature of the nanoparticles. The lattice fringes clearly observed and the spacing of the two neighbouring plane is about 0.12 nm, which is consist with the interplanar separation of the (200) plane in cubic (fcc) Ni. The HRTEM image of a single Ni nanoparticles showed that the nanoparticles were highly crystalline (Fig. 3c).

Fig. 4 is the UV-vis spectrum of the as-synthesized NiO nanoparticles dispersed in ethanol. A strong absorption in the UV region is observed at wavelengths about 362 nm. The strong absorption in the UV region is attributed to band gap absorption in NiO [31]. It is well known that optical band gap ( $E_g$ ) can be calculated on the basis of the optical absorption spectrum by the following equation:

$$(Ah\nu)^n = B(h\nu - E_g)$$

where  $h\nu$  is the photo energy,  $A$  is absorbance,  $B$  is a constant relative to the material and  $n$  is either two for direct transition or 1/2 for an indirect transition [32]. Hence, the optical band gap for the absorption peak can be obtained by extrapolating the linear portion of the  $(Ah\nu)^n - h\nu$  curve to zero. The band gap of the NiO particles is about 3.42 eV, which is similar to the value (3.55 eV) reported by Boschloo and Hagfeldt [33]. No linear relation was found for  $n=1/2$ , suggesting that the as-prepared NiO nanoparticles are semiconducting with direct transition at this energy [31].

The magnetic property of Ni nanoparticles has been measured (Fig. 5a). The saturation magnetization ( $M_s$ ) for the nanospheres samples is 54.2 emu g<sup>-1</sup> (1 emu g<sup>-1</sup> = 1 A m<sup>2</sup> kg<sup>-1</sup>) which is close to that of bulk Ni (ca. 55 Oe (1 Oe = 79.6 A m<sup>-2</sup>)). Coercivity field ( $H_c$ ) of Ni nanoparticles is about (19.4 Oe). Compared with the corresponding value for bulk Ni (0.7 Oe), the coercivities of the Ni nanoparticles clearly show significant enhancement. This enhancement can likely be attributed to the reduced particle sizes of obtained product [34] which change the magnetization reversal mechanism. This demonstrates that the magnetic properties of the Ni nanoparticles are greatly influenced by their microstructure. As shown in Fig. 5a, the hysteresis loop is symmetric with respect to zero magnetic fields, indicating that there is no exchange biasing effect, which is usually caused by the presence of NiO [35,36]. Fig. 5b shows the hysteresis loops of NiO nanoparticles at 300 K. It can be seen that NiO nanoparticles present a superparamagnetic behavior although NiO bulk material is antiferromagnetic [37].

#### 4. Conclusion

Nanoparticles of Ni and NiO with average particle sizes of 14–22 nm from thermal decomposition of [bis(2-hydroxyacetophenato)nickel(II)] as precursor have been synthesized. The XRD pattern of the fresh nickel nanoparticles, showed the fcc structure of nickel. The optical absorption band gap of the nickel oxide nanoparticles was estimated to be 3.42 eV.

#### Acknowledgement

Authors are grateful to council of University of Kashan for providing financial support to undertake this work.

#### References

- [1] Y. Yin, A.P. Alivisatos, Nature 437 (2005) 664–670.
- [2] T. Neuberger, B. Scopf, H. Hofmann, M. Hofmann, B.V. Rechenberg, J. Magn. Mater. 293 (2005) 483–496.
- [3] D.J. Schiffrin, MRS Bull. 26 (2001) 1015–1019.
- [4] S. Hironari, Y. Nakano, H. Matsushita, A. Onoe, H. Kanai, Y. Yamashita, J. Mater. Synth. Process. 6 (1998) 415–420.
- [5] E. Antolini, M. Ferretti, S. Gemme, J. Mater. Sci. 31 (1996) 2187–2192.
- [6] B.C. Gates, Chem. Rev. 95 (1995) 511–522.

- [7] L.N. Lewis, *Chem. Rev.* 93 (1993) 2693–2730.
- [8] L.L. Beecroft, C.K. Ober, *Chem. Mater.* 9 (1997) 1302–1317.
- [9] S. Morup, in: A. Hernando (Ed.), *Studies of Superparamagnetism in Samples of Ultrafine Particles, Nanomagnetism*, Kluwer Academic Publishers, Boston, 1993, pp. 93–99.
- [10] A. Aharoni, *Introduction to the Theory of Ferromagnetism*, Oxford University Press, New York, 1996, pp. 133–152.
- [11] L. Babes, B. Denizot, G. Tanguy, J.J. Le Jeune, P. Jallet, *J. Colloids Interf. Sci.* 212 (1999) 474–482.
- [12] U. Hafeli, W. Schutt, J. Teller, M. Zborowski (Eds.), *Scientific and Clinical Applications of Magnetic Carriers*, Plenum Press, New York, 1997.
- [13] I. Safarik, M. Safarikova, *Monatsh. Chem.* 133 (2002) 737–759.
- [14] Y. Hou, H. Kondoh, T. Ohta, S. Gao, *Appl. Surf. Sci.* 241 (2005) 218–222.
- [15] N. Cordente, C. Amiens, B. Chaudret, M. Respaud, F. Senocq, M.J. Casanove, *J. Appl. Phys.* 94 (2003) 6358–6365.
- [16] T. Ould-Ely, C. Amiens, B. Chaudret, E. Snoeck, M. Verelst, M. Respaud, J.M. Broto, *Chem. Mater.* 11 (1999) 526–529.
- [17] J. Gong, L.L. Wang, Y. Liu, J.H. Yang, Z.G. Zong, *J. Alloys Compd.* 457 (2008) 6–9.
- [18] C.B. Murray, S. Sun, H. Doyle, T. Bettley, *MRS Bull.* 26 (2001) 985–991.
- [19] S.R. Hoon, M. Kilner, G.J. Russell, B.K. Tanner, *J. Magn. Magn. Mater.* 39 (1983) 107–110.
- [20] D. de Caro, J.S. Bradley, *Langmuir* 13 (1997) 3067–3067.
- [21] T.O. Ely, C. Amiens, B. Chaudret, E. Snoeck, M. Verelst, M. Respaud, J.M. Broto, *Chem. Mater.* 11 (1999) 526–529.
- [22] X. Wang, J. Song, L. Gao, J. Jin, H. Zheng, Z. Zhang, *Nanotechnology* 16 (2005) 37–39.
- [23] H.T. Zhang, G. Wu, X.H. Chen, X.G. Qiu, *Mater. Res. Bull.* 41 (2006) 495–501.
- [24] J. Park, E. Kang, S.U. Son, H.M. Park, M.K. Lee, J. Kim, K.W. Kim, H.J. Noh, J.H. Park, C.J. Bae, J.G. Park, T. Hyeon, *Adv. Mater.* 17 (2005) 429–434.
- [25] T. Hyeon, S.S. Lee, J. Park, Y. Chung, H.B. Na, *J. Am. Chem. Soc.* 123 (2001) 12798–12801.
- [26] M. Salavati-Niasari, F. Davar, M. Mazaheri, M. Shaterian, *J. Magn. Magn. Mater.* 320 (2008) 575–578.
- [27] M. Salavati-Niasari, F. Davar, M. Mazaheri, *Mater. Lett.* 62 (2008) 1890–1892.
- [28] M. Salavati-Niasari, M. Shaterian, M.R. Ganjali, P. Norouzi, *J. Mol. Catal. A: Chem.* 261 (2007) 147–155.
- [29] C. Mui, J. Han, G. Wang, C. Musgrave, S. Bent, *J. Am. Chem. Soc.* 124 (2002) 4027–4038.
- [30] M. Kanthimathi, A. Dhathathreyan, B.V. Nair, *Mater. Lett.* 58 (2004) 2914–2917.
- [31] X. Li, X. Zhang, Z. Li, Y. Qian, *Solid State Commun.* 137 (2006) 581–584.
- [32] A. Hagfeldt, M. Gratzel, *Chem. Rev.* 95 (1995) 49–68.
- [33] G. Boschloo, A. Hagfeldt, *J. Phys. Chem. B* 105 (2001) 3039–3044.
- [34] J.H. Hwang, V.P. Dravid, M.H. Teng, J.J. Host, B.R. Elliott, D.L. Johnson, T.O. Mason, *J. Mater. Res.* 12 (1997) 1076–1082.
- [35] C. Liu, L. Guo, R. Wang, Y. Deng, H. Xu, S. Yang, *Chem. Commun.* (2004) 2726–2727.
- [36] J. Nogués, I.K. Schuller, *J. Magn. Magn. Mater.* 192 (1999) 203–232.
- [37] P. Ngo, P. Bonville, M.P. Pileni, *Eur. Phys. J. B* 9 (1999) 583–593.